

# Draft genomes of a male and female Australian jacky dragon

(*Amphibolurus muricatus*)

Ran Tian<sup>1,2</sup>, Han Guo<sup>1</sup>, Chen Yang<sup>1</sup>, Guangyi Fan<sup>3,4</sup>, Sarah L. Whiteley<sup>5,6</sup>, Clare E. Holleley<sup>6</sup>, Inge Seim<sup>1,7</sup>, Arthur Georges<sup>5,8\*</sup>

<sup>1</sup> Integrative Biology Laboratory, College of Life Sciences, Nanjing Normal University, Nanjing 210046, China

<sup>2</sup> Jiangsu Key Laboratory for Biodiversity and Biotechnology, College of Life Sciences, Nanjing Normal University, Nanjing 210046, China

<sup>3</sup> BGI-Qingdao, Qingdao 266555, China

<sup>4</sup> BGI-Shenzhen, Shenzhen 518083, China

<sup>5</sup> Institute for Applied Ecology, University of Canberra, Canberra 2617, Australia

<sup>6</sup> Australian National Wildlife Collection, CSIRO, Canberra 2601, Australia

<sup>7</sup> School of Biology and Environmental Science, Queensland University of Technology, Brisbane 4000, Australia

<sup>8</sup> AusARG consortium, Bioplatforms Australia, Research Park Drive, Macquarie University, Macquarie Park 2109, Australia

\* Corresponding author: Institute for Applied Ecology, University of Canberra, ACT 2601, Australia. E-mail: georges@aerg.canberra.edu.au

1 **ABSTRACT**

2 Australia is remarkable for its lizard diversity, with very high endemism because of  
3 continental-scale diversification and adaptive radiation. We employed 10X Genomics  
4 Chromium linked-reads technology to generate male and female draft genomes of the jacky  
5 dragon (*Amphibolurus muricatus*), an Australian dragon lizard (family Agamidae). The  
6 assemblies are 1.8 Gb in size and have a repeat content (38%) and GC content (42%) similar  
7 to other dragon lizards. The contig N50 values for the assemblies were 37.2 kb (female) and  
8 28.8 kb (male), with corresponding scaffold N50 values of 720.5 kb and 369 kb. The longest  
9 scaffold was 6.5 Mb in each assembly. The BUSCO completeness percentages were 92.2%  
10 and 90.8% respectively. These statistics are comparable to other lizard genomes assembled  
11 using similar technology. Phylogenetic comparisons show that Australian dragon lizard  
12 species split from a common ancestor around 33.4 million years ago. The draft *A. muricatus*  
13 assemblies will be a valuable resource for understanding lizard sex determination and the  
14 evolution and conservation of Australian dragon lizards.

15

16 **Keywords:** agamid lizard; Agamidae; squamate; nuclear genome; genome assembly

17

18

19

20

## 21 **Introduction**

22 The Australian jacky dragon, *Amphibolurus muricatus* (**Figure 1**), is lizard widespread in dry  
23 sclerophyll forests of south-eastern and eastern Australia (Cogger, 2014). It is a model  
24 species for biogeography (Pepper et al., 2014), evolutionary biology (Warner and Shine,  
25 2008; Warner et al., 2013), social behaviour (Peters and Evans, 2003; Woo and Rieucou,  
26 2013), and development (Esquerré et al., 2014; Whiteley et al., 2021).

27 Species in the genus *Amphibolurus* and *Chlamydosaurus* are a major clade in the  
28 Australian radiation of the Agamidae (Hugall et al., 2008). The draft assembly of *A.*  
29 *muricatus*, together with that of *Pogona vitticeps* (Georges et al., 2015), represents the first  
30 foray into generating the necessary high-quality genomes for the Agamidae. In particular,  
31 *A. muricatus* occupies mesic habitats and so is intermediate between the Australian water  
32 dragon *Intellagama lesueurii* and the forest dragon *Lophosaurus boydii* that occupy hydric  
33 habitats and the central bearded dragon *Pogona vitticeps* and the Lake Eyre dragon  
34 *Ctenophorus maculosus*, for example, that occupy more xeric habitats. As such, it is one of  
35 several species important for understanding genomic adaptation to the progressive aridity that  
36 has occurred in Australia in the past 15 Myr. *Amphibolurus muricatus* is also of particular  
37 interest because it has temperature-dependent sex determination (TSD) (Harlow and Taylor,  
38 2000) and it is unclear as to whether this arises from classical TSD or a combination of  
39 genetic and environmental influences (Whiteley et al. 2021). Studies of the underlying  
40 mechanisms of TSD require a genome assembly and knowledge of genome organisation to  
41 identify genes on the sex chromosomes of species with genotypic sex determination (GSD)  
42 and their chromosomal and gene homology in closely related TSD species. This is  
43 particularly so in species with TSD that show evidence of cryptic residual or de novo  
44 genotypic influence on offspring sex ratios, as is suspected for *A. muricatus* (Whiteley et al.,  
45 2021).

46 Here, we employ high-throughput linked-read sequencing (10X Genomics) (Zheng et  
47 al., 2016) to generate draft, annotated genome assemblies for a male and a female *A.*  
48 *muricatus* that are comparable in contiguity and completeness to other published Agamid  
49 genomes generated using Illumina short-read technologies (Georges et al., 2015). We used  
50 transcriptomes sequenced and assembled for *A. muricatus* and published assemblies (*Anolis*,  
51 *Varanus*, *Pogona*) to annotate the genomes. Our assemblies will provide a resource to  
52 increase capacity and accelerate the progress of studies into the evolution, ecology, and  
53 conservation of Australian dragon lizards.

54

## 55 **Materials and methods**

56

### 57 **Sample collection**

58 To reduce the high heterozygosity that presented difficulties in the assembly of the genome of  
59 *Pogona vitticeps* (Georges et al., 2015), we generated inbred lines of *A. muricatus*. The  
60 founding male and female pair were sourced from the wild and bred in captivity. The two  
61 animals used to generate the genome were obtained from the fourth generation of the inbred  
62 pedigree produced by sib-sib matings and back crossing (see **Figure S1** for the complete  
63 pedigree). The male (AA069033) and female (AA069032) individual used for the genome  
64 and transcriptome sequencing were humanely euthanised via intraperitoneal injection of  
65 sodium pentobarbitone (60 mg/ml in isotonic saline). Organs were rapidly dissected and snap  
66 frozen in liquid nitrogen.

67

### 68 **Linked-read whole-genome sequencing and de novo assembly**

69 High molecular weight DNA was extracted from liver (female) and blood (male) using the  
70 Genra Puregene DNA Isolation kit (Qiagen). DNA yield and quality was assessed using a  
71 NanoDrop spectrophotometer (Thermo Fisher Scientific, Waltham, MA, USA) and a Qubit  
72 fluorometer (Thermo Fisher Scientific). Male and female *A. muricatus* genome sequencing  
73 libraries were constructed on the Chromium system (10X Genomics, Pleasanton, CA, USA)  
74 by the Ramaciotti Centre for Genomics (Sydney, Australia). The Chromium instrument  
75 enables unique barcoding of long stretches of DNA on gel beads. The barcodes allow later  
76 reconstruction of long DNA fragments from a series of short DNA fragments with the same  
77 barcode (i.e. linked-reads). After barcoding, DNA was sheared into smaller fragments and  
78 sequenced on the NovaSeq 6000 platform (Illumina, CA, USA) to generate 151 bp paired-  
79 end (PE) reads. A total of 904.9 M raw 10X Genomics Chromium linked-reads were  
80 generated.

81 To estimate the genome sizes and heterozygosity of the female and male *A. muricatus*  
82 samples, we used GenomeScope (Vurture et al., 2017). Briefly, we employed KmerGenie  
83 v1.7051 (Chikhi and Medvedev, 2014) and short-read sequencing data (paired-ends reads  
84 generated above) to determine the optimal  $k$ -mer-value range, indicating that a minimum  $k$ -  
85 mer length of 31 and 41 for the male and female, respectively. Next,  $k$ -mers in the paired-end  
86 sequencing reads were counted and converted to histogram files using Jellyfish (v2.2.10)  
87 (Marcais and Kingsford, 2011), followed by analysis using GenomeScope v1.0.

88 Raw 10X data were assembled with Supernova v2.1.1 (Weisenfeld et al., 2017) and a  
89 FASTA file was generated using the ‘pseudohap style’ option in Supernova mkoutput. All  
90 female (~450 M) and male (~550 M) read pairs were utilised (female sequencing depth *ca*  
91 50.3x; male, *ca* 47.8x). The resulting assembly was further scaffolded with ARKS v1.0.3  
92 (Coombe et al., 2018), reusing the 10X reads, and the companion LINKS program (v1.8.7)  
93 (Warren et al., 2015). ARKS employs a *k*-mer approach to map linked barcodes to the contigs  
94 in the initial Supernova assembly to generate a scaffold graph with estimated distances for  
95 LINKS input. Next, RNA-seq reads (from brain, ovary, and testis; see below) were filtered  
96 (i.e. cleaned) to remove adapters and low-quality reads using Flexbar v3.4.0 and used to  
97 further re-scaffold the assembly with P\_RNA\_scaffolder (Zhu et al., 2018). The default  
98 Flexbar settings discards all reads with any uncalled bases. A final round of scaffolding was  
99 performed on the resulting assembly using L\_RNA\_scaffolder (Xue et al., 2013). We used  
100 GapCloser v1.12 (part of SOAPdenovo2) (Luo et al., 2012) to fill gaps in the assembly.  
101 GapCloser was run using the parameter -l 150) and cleaned 10X Genomics reads PE reads.  
102 Genome assemblies were assessed using BUSCO 5.0.0\_cv1 (Seppey et al., 2019).

103

#### 104 **RNA-seq and transcriptome assembly**

105 Raw data 125 bp PE reads, generated on an Illumina HiSeq 2500 instrument was filtered  
106 using Flexbar v3.4.0 (Dodt et al., 2012; Roehr et al., 2017) with default settings (removes  
107 reads with any uncalled bases). Any residual ribosomal RNA reads (the majority removed by  
108 poly(A) selection prior to sequencing library generation) were removed using SortMeRNA  
109 v2.1b (Kopylova et al., 2012) against the SILVA v119 ribosomal database (Quast et al.,  
110 2013). Tissue transcriptomes were de novo assembled using Trinity v2.11.0 (Grabherr et al.,  
111 2011; Haas et al., 2013; Henschel et al., 2012) and assessed using BUSCO 5.0.0\_cv1 (Seppey  
112 et al., 2019).

113

#### 114 **Genome annotation**

115 We identified repetitive elements by integrating homology and de novo prediction data.  
116 Protein-coding genes were annotated using homology-based prediction, de novo prediction,  
117 and RNA-seq-assisted prediction methods.

118 Homology-based transposable elements (TE) annotations were obtained by  
119 interrogating a genome assembly with known repeats in the Repbase database v16.02 (Bao et  
120 al., 2015) using RepeatMasker v4.0.5 (DNA-level) (Tarailo-Graovac and Chen, 2009) and  
121 RepeatProteinMask (protein-level; implemented in RepeatMasker). De novo TE predictions

122 were obtained using RepeatModeler v1.1.0.4 (Smit and Hubley, 2010) and LTRharvest  
123 v1.5.8 (Ellinghaus et al., 2008) to generate database for a RepeatMasker run. Tandem Repeat  
124 Finder (v4.07) (Benson, 1999) was used to find tandem repeats (TRs) in the genome. A non-  
125 redundant repeat annotation set was obtained by combining the above data.

126 Protein-coding genes were annotated using homology-based prediction, de novo  
127 prediction, and RNA-seq-assisted [generated from ovary, testis, and brain (both sexes)]  
128 prediction methods. Sequences of homologous proteins from three lizards [*Anolis*  
129 *carolinensis* (green anole) assembly AnoCar2.0 (RefSeq assembly GCF\_000090745.1)  
130 (Alfoldi et al., 2011); *Varanus komodoensis* (Komodo dragon) assembly ASM479886v1  
131 (GCA\_004798865.1) (Lind et al., 2019); and *Pogona vitticeps* (central bearded dragon)  
132 assembly pvi1.1 (GCF\_900067755.1)] (Georges et al., 2015) were downloaded from NCBI.  
133 These protein sequences were aligned to the repeat-masked genome using BLAT v0.36  
134 (Kent, 2002). GeneWise v2.4.1 (Birney et al., 2004) was employed to generate gene  
135 structures based on the alignments of proteins to a genome assembly. De novo gene  
136 prediction was performed using AUGUSTUS v3.2.3 (Stanke et al., 2006), GENSCAN v1.0  
137 (Burge and Karlin, 1997), and GlimmerHMM v3.0.1 (Majoros et al., 2004) with a human  
138 training set. Transcriptome data (cleaned reads) were mapped to the assembled genome using  
139 HISAT2 v2.1.0 (Kim et al., 2019) and SAMtools v1.9 (Li et al., 2009), and coding regions  
140 were predicted using TransDecoder v5.5.0 (Grabherr et al., 2011; Haas et al., 2013). A final  
141 non-redundant reference gene set was generated by merging the three annotated gene sets  
142 using EvidenceModeler v1.1.1 (EVM) (Haas et al., 2008) and excluding EVM gene models  
143 with only ab initio support. The gene models were translated into amino acid sequences and  
144 used in local BLASTp (Camacho et al., 2009) searches against the public databases Kyoto  
145 Encyclopedia of Genes and Genomes (KEGG; v89.1) (Kanehisa and Goto, 2000), NCBI non-  
146 redundant protein sequences (NR; v20170924) (O'Leary et al., 2016), Swiss-Prot (release-  
147 2018\_07) (UniProt Consortium, 2012), TrEMBL (Translation of EMBL [nucleotide  
148 sequences that are not in Swiss-Prot]; release-2018\_07) (O'Donovan et al., 2002), and  
149 InterPro (v69.0) (Mitchell et al., 2019).

150

### 151 **Phylogeny and divergence time estimation**

152 In addition to *A. carolinensis*, *V. komodoensis*, and *P. vitticeps* (see section above), the  
153 genome and sequences of homologous proteins from *Gekko japonicus* (Schlegel's Japanese  
154 gecko) assembly Gekko\_japonicus\_V1.1 (GCA\_001447785.1) (Liu et al., 2015) and  
155 *Crotalus tigris* (tiger rattlesnake) assembly ASM1654583v1 (GCA\_016545835.1) (Margres

156 et al., 2021) were downloaded from NCBI. The genome and annotations of *Ophisaurus*  
157 *gracilis* (Anguidae lizard) were downloaded from GigaDB (Song et al., 2015a; Song et al.,  
158 2015b). No gene annotation data was available for three species: *Intellagama lesueurii*  
159 (Australian water dragon; assembly EWD\_hifiasm\_HiC generated as part of the AusARG  
160 consortium and (downloaded from DNA Zoo (Cheng et al., 2021; Dudchenko et al., 2017;  
161 Dudchenko et al., 2018)) and the Chinese agamid lizards *Phrynocephalus przewalskii*  
162 (Przewalski's toadhead agama) (Gao et al., 2019) and *Phrynocephalus vlangalii* (Ching Hai  
163 toadhead agama) (Gao et al., 2019) (CNCBdb accession no. CNP0000203). Their protein-  
164 coding genes were annotated using homology-based prediction, de novo prediction, and  
165 RNA-seq-assisted prediction methods (see genome annotation section above).

166 We identified 4,242 high-confidence 1:1 orthologs by interrogating the predicted  
167 proteins from the gene models of ten species using SonicParanoid v1.3.0 (Cosentino and  
168 Iwasaki, 2019). The corresponding coding sequences (CDS) for each species were aligned  
169 using PRANK v100802 (Loytynoja and Goldman, 2005) and filtered by Gblocks v0.91b  
170 (Talavera and Castresana, 2007) to identify conserved blocks (removing gaps, ambiguous  
171 sites, and excluding alignments less than 300 bp in size), leaving 4,242 genes. Maximum-  
172 likelihood (ML) phylogenetic trees were generated using RaxML v7.2.8 (Stamatakis, 2006)  
173 and IQ-Tree v2.1.3 (Minh et al., 2020) with three CDS data sets: the whole coding sequence  
174 (whole-CDS), first codon positions, and fourfold degenerate (4d) sites. Identical topologies  
175 and similar support values were obtained (1,000 bootstrap iterations were performed). The  
176 divergence time between species was estimated using MCMCTree [a Bayesian molecular  
177 clock model implemented in PAML v4.7 (Yang, 2007)] with the JC69 nucleotide substitution  
178 model, and the whole-CDS ML tree and concatenated whole-CDS supergenes as inputs. We  
179 used 100,000 iterations after a burn-in of 10,000 iterations. MCMCTree calibration points  
180 (million years ago; Mya) were obtained from TimeTree (Kumar et al., 2017): *G. japonicus*-*P.*  
181 *przewalskii* (190-206 Mya), *V. komodoensis*-*O. gracilis* (121-143 Mya), *V. komodoensis*-*C.*  
182 *tigris* (156-174 Mya), *V. komodoensis*-*A. carolinensis* (155-175 Mya), *I. lesueurii*-*A.*  
183 *carolinensis* (139-166 Mya), *I. lesueurii*-*P. przewalskii* (73-93 Mya), *I. lesueurii*-*A.*  
184 *muricatus* (25.5-42.4 Mya), *P. vitticeps*-*A. muricatus* (20.2-34.6 Mya).

## 185 **Results and discussion**

186

### 187 **Draft genome assembly and comparisons with other squamates**

188 We used GenomeScope (Vurture et al., 2017) to obtain a *k*-mer-based estimate of genome  
189 size and heterozygosity from paired-end sequence reads. The size of the *A. muricatus* genome  
190 is estimated to be around 1.8 Gb (**Figure S2**). The genome-wide heterozygosity from our  
191 inbred *A. muricatus* lines was estimated to range from 0.58% (female) to 0.78% (male)  
192 (**Figure S2**), slightly lower than the central bearded dragon (*Pogona vitticeps*) (0.85%)  
193 (Georges et al., 2015).

194 10X Genomics sequencing data were assembled into contigs, then oriented and  
195 merged into scaffolds. Combining ARKS and P\_RNA\_scaffolder (employs RNA-seq reads  
196 from brain, ovary, and testis) (**Table S1**) and L\_RNA\_scaffolders (employs Trinity  
197 transcriptome assemblies) (**Tables S2 and S3**), the scaffold N50 size of the female *A.*  
198 *muricatus* (named AmuF1.1) assembly improved by 38.3% (from 371.5 kb to 720.5 kb),  
199 while the BUSCO completeness percentage improved from 84.1% to 92.2% (**Table S4**). The  
200 male assembly (AmuM1.1) saw a similar improvement, with the scaffold N50 and BUSCO  
201 score increasing from 180.2 kb to 369.9 kb and from 78.9% to 90.8%, respectively. The final  
202 assemblies had a total scaffold length (contain gaps) of 1.84 Gb (female) and 1.83 Gb (male)  
203 with a longest scaffold *ca* 6.5 Mb in each assembly (**Table 1**). The contig N50 values for the  
204 assemblies were 37.2 kb (female) and 28.8 kb (male). The scaffold and contig N50 values are  
205 similar to those of other squamate genome assemblies (**Figure 2**), with the exception of the  
206 chromosome-assigned assemblies of Australian water dragon (*Intellagama lesueurii*; scaffold  
207 N50 268.9 Mb), tiger rattlesnake (*Crotalus tigris*; scaffold N50 2.1 Mb) (Margres et al.,  
208 2021), green anole (*Anolis carolinensis*; scaffold N50 150.1 Mb), and Komodo dragon  
209 (*Varanus komodoensis*; scaffold N50 23.8 Mb) (Lind et al., 2019). The BUSCO metrics of  
210 the *A. muricatus* assemblies indicate that they compare well to other squamate assemblies,  
211 including agamids from Australia [*P. vitticeps* (Georges et al., 2015) and *I. lesueurii*  
212 (Australian water dragon)] and China (toad-headed agamas of genus *Phrynocephalus* sp.  
213 (Gao et al., 2019)) (**Figure 3**) and **Table S5**).

214

### 215 **Genome annotation**

216 The *A. muricatus* assemblies are composed of 38% repeat elements and have a GC content of  
217 42% (**Tables S4 and S6**), similar to that of *P. vitticeps* (Georges et al., 2015) – with LINES  
218 being the predominant subtype. Protein-coding genes were annotated by combining



219 transcriptome evidence with homology-based (*A. carolinensis*, *V. komodoensis*, and *P.*  
220 *vitticeps*) and de novo gene prediction methods. Gene statistics (**Table S8**) (see (Georges et  
221 al., 2015)) and gene set BUSCO scores (**Table S9**) are comparable to other squamates. Using  
222 ab initio, transcriptome, and homology-based prediction methods, we functionally annotated  
223 18,197 (85.0%) and 17,360 (88.0%) protein-coding genes in the female and male assembly  
224 (**Tables S10 and S11**) and recovered 94.7% and 93.1% of 3,354 vertebrate benchmarking  
225 universal single-copy orthologs (BUSCOs) (Seppey et al., 2019), respectively.

226

### 227 **Phylogenetic relationships**

228 To construct a time-calibrated species tree (**Figure 4**), we identified 4,242 high-confidence  
229 single-copy orthologs from the female *A. muricatus* assembly and nine other squamate  
230 species. There are currently five agamid lizard genome assemblies: three Australian dragon  
231 lizard assemblies (*A. muricatus*, *P. vitticeps*, and *I. lesueurii*) and two toad-headed agama  
232 assemblies (genus *Phrynocephalus*) (Gao et al., 2019; Georges et al., 2015). Our analysis  
233 shows that the five agamid species shared an ancestor about 85.7 Mya [81.3-88.2 Mya 95%  
234 credibility interval (CI)]. We estimate that the three Australian dragon lizard species split  
235 from a common ancestor about 33.4 Mya (95% CI 28.8-39.1), while the lineages leading to  
236 *A. muricatus* and *P. vitticeps* diverged 23.6 Mya (95% CI 19.4-28.2). These observations are  
237 in agreement with an appraisal from a small set of mitochondrial and nuclear genes (Hugall et  
238 al., 2008).

239

### 240 **Conclusions and perspectives**

241 In this study, we generated the first annotated genome assemblies of *Amphibolurus*  
242 *muricatus*. Overall, the assemblies are similar in quality to a range of squamate genomes and  
243 will be immediately useful for researchers. Nevertheless, it is appreciated that the assemblies  
244 can be further improved. Such efforts will be particularly important for future studies on  
245 squamate chromosome evolution and sex determination. Single-tube Long Fragment Read  
246 (stLFR) sequencing (Fan et al., 2019; Wang et al., 2019) and re-scaffolding using SLR-  
247 superscaffolder (Guo et al., 2021), and chromatin conformation capture (Hi-C) (Lieberman-  
248 Aiden et al., 2009) sequencing to generate a chromosome-level assembly is planned by the  
249 AusARG initiative of Bioplatforms Australia (<https://bioplatforms.com>). In conclusion, the *A.*  
250 *muricatus* assemblies described here should prove valuable for the understanding of agamid  
251 lizard evolution, ecology, and conservation.

252 **Data availability**

253 *A. muricatus* raw genome and transcriptome reads have been deposited to the NCBI Short  
254 Read Database (BioProject ID: PRJNA767251). The male and female *A. muricatus*  
255 assemblies are available at Zenodo (Tian et al., 2021b). Gene annotation files and associated  
256 FASTA files for *A. muricatus* (assembly AmuF1.1), *I. lesueurii*, *P. przewalskii*, and *P.*  
257 *vlangalii* are available at Zenodo (Tian et al., 2021c). *A. muricatus* transcriptome assemblies  
258 are available at Zenodo (Tian et al., 2021a). Various scripts used for data processing and  
259 analyses are available on GitHub at <https://github.com/sciseim/JackyDragon>.

260

261 **Acknowledgements**

262 We thank Dr Wendy Ruscoe and Jacqui Richardson for their assistance in generating the  
263 inbred line of *A. muricatus* and for animal husbandry.

264

265 **Conflict of interest**

266 The authors declare there is no conflict of interest.

267

268 **Ethics Approvals**

269 All sampling and breeding experiments were conducted with approval of the Animal Ethics  
270 Committee of the University of Canberra and in accordance with their Standard Operating  
271 Procedures.

272

273 **Funding**

274 Financial support for this work was provided by an Australian Research Council Discovery  
275 Grant (DP170101147; to A.G. and C.E.H.), a specially-appointed Professor of Jiangsu  
276 Province grant (to I.S.), the Jiangsu Science and Technology Agency (to I.S.), and the Jiangsu  
277 Foreign Expert Bureau (to I.S.).

278

279 **Literature cited**

280 Alföldi, J., Di Palma, F., Grabherr, M., Williams, C., Kong, L., Mauceli, E., Russell, P.,  
281 Lowe, C.B., Glor, R.E., Jaffe, J.D., *et al.* (2011). The genome of the green anole lizard and a  
282 comparative analysis with birds and mammals. *Nature* 477, 587-591.  
283 Bao, W., Kojima, K.K., and Kohany, O. (2015). Repbase Update, a database of repetitive  
284 elements in eukaryotic genomes. *Mob DNA* 6, 11.  
285 Benson, G. (1999). Tandem repeats finder: a program to analyze DNA sequences. *Nucleic*  
286 *Acids Res* 27, 573-580.

287 Birney, E., Clamp, M., and Durbin, R. (2004). GeneWise and Genomewise. *Genome Res* 14,  
288 988-995.

289 Burge, C., and Karlin, S. (1997). Prediction of complete gene structures in human genomic  
290 DNA. *J Mol Biol* 268, 78-94.

291 Camacho, C., Coulouris, G., Avagyan, V., Ma, N., Papadopoulos, J., Bealer, K., and Madden,  
292 T.L. (2009). BLAST+: architecture and applications. *BMC Bioinformatics* 10, 421.

293 Cheng, H., Concepcion, G.T., Feng, X., Zhang, H., and Li, H. (2021). Haplotype-resolved de  
294 novo assembly using phased assembly graphs with hifiasm. *Nat Methods* 18, 170-175.

295 Chikhi, R., and Medvedev, P. (2014). Informed and automated k-mer size selection for  
296 genome assembly. *Bioinformatics* 30, 31-37.

297 Cogger, H. (2014). *Reptiles and amphibians of Australia* (CSIRO publishing).

298 Coombe, L., Zhang, J., Vandervalk, B.P., Chu, J., Jackman, S.D., Birol, I., and Warren, R.L.  
299 (2018). ARKS: chromosome-scale scaffolding of human genome drafts with linked read  
300 kmers. *BMC Bioinformatics* 19, 234.

301 Cosentino, S., and Iwasaki, W. (2019). SonicParanoid: fast, accurate and easy orthology  
302 inference. *Bioinformatics* 35, 149-151.

303 Dodt, M., Roehr, J.T., Ahmed, R., and Dieterich, C. (2012). FLEXBAR-Flexible Barcode  
304 and Adapter Processing for Next-Generation Sequencing Platforms. *Biology (Basel)* 1, 895-  
305 905.

306 Dudchenko, O., Batra, S.S., Omer, A.D., Nyquist, S.K., Hoeger, M., Durand, N.C., Shamim,  
307 M.S., Machol, I., Lander, E.S., Aiden, A.P., *et al.* (2017). De novo assembly of the *Aedes*  
308 *aegypti* genome using Hi-C yields chromosome-length scaffolds. *Science* 356, 92-95.

309 Dudchenko, O., Shamim, M.S., Batra, S.S., Durand, N.C., Musial, N.T., Mostofa, R., Pham,  
310 M., St Hilaire, B.G., Yao, W., and Stamenova, E. (2018). The Juicebox Assembly Tools  
311 module facilitates de novo assembly of mammalian genomes with chromosome-length  
312 scaffolds for under \$1000. *BioRxiv*, 254797.

313 Ellinghaus, D., Kurtz, S., and Willhoeft, U. (2008). LTRharvest, an efficient and flexible  
314 software for de novo detection of LTR retrotransposons. *BMC Bioinformatics* 9, 18.

315 Esquerré, D., Keogh, J.S., and Schwanz, L.E. (2014). Direct effects of incubation temperature  
316 on morphology, thermoregulatory behaviour and locomotor performance in jacky dragons  
317 (*Amphibolurus muricatus*). *Journal of Thermal Biology* 43, 33-39.

318 Fan, H., Wu, Q., Wei, F., Yang, F., Ng, B.L., and Hu, Y. (2019). Chromosome-level genome  
319 assembly for giant panda provides novel insights into Carnivora chromosome evolution.  
320 *Genome Biol* 20, 267.

321 Gao, W., Sun, Y.B., Zhou, W.W., Xiong, Z.J., Chen, L., Li, H., Fu, T.T., Xu, K., Xu, W., Ma,  
322 L., *et al.* (2019). Genomic and transcriptomic investigations of the evolutionary transition  
323 from oviparity to viviparity. *Proc Natl Acad Sci U S A* 116, 3646-3655.

324 Georges, A., Li, Q., Lian, J., O'Meally, D., Deakin, J., Wang, Z., Zhang, P., Fujita, M., Patel,  
325 H.R., Holleley, C.E., *et al.* (2015). High-coverage sequencing and annotated assembly of the  
326 genome of the Australian dragon lizard *Pogona vitticeps*. *Gigascience* 4, 45.

327 Grabherr, M.G., Haas, B.J., Yassour, M., Levin, J.Z., Thompson, D.A., Amit, I., Adiconis,  
328 X., Fan, L., Raychowdhury, R., Zeng, Q., *et al.* (2011). Full-length transcriptome assembly  
329 from RNA-Seq data without a reference genome. *Nat Biotechnol* 29, 644-652.

330 Guo, L., Xu, M., Wang, W., Gu, S., Zhao, X., Chen, F., Wang, O., Xu, X., Seim, I., Fan, G.,  
331 *et al.* (2021). SLR-superscaffolder: a de novo scaffolding tool for synthetic long reads using a  
332 top-to-bottom scheme. *BMC Bioinformatics* 22, 158.

333 Haas, B.J., Papanicolaou, A., Yassour, M., Grabherr, M., Blood, P.D., Bowden, J., Couger,  
334 M.B., Eccles, D., Li, B., Lieber, M., *et al.* (2013). De novo transcript sequence reconstruction  
335 from RNA-seq using the Trinity platform for reference generation and analysis. *Nat Protoc* 8,  
336 1494-1512.

337 Haas, B.J., Salzberg, S.L., Zhu, W., Pertea, M., Allen, J.E., Orvis, J., White, O., Buell, C.R.,  
338 and Wortman, J.R. (2008). Automated eukaryotic gene structure annotation using  
339 EVIDENCEModeler and the Program to Assemble Spliced Alignments. *Genome Biol* 9, R7.  
340 Harlow, P.S., and Taylor, J.E. (2000). Reproductive ecology of the jacky dragon  
341 (*Amphibolurus muricatus*): an agamid lizard with temperature-dependent sex determination.  
342 *Austral Ecology* 25, 640-652.

343 Henschel, R., Lieber, M., Wu, L.-S., Nista, P.M., Haas, B.J., and LeDuc, R.D. (2012). Trinity  
344 RNA-Seq assembler performance optimization. Paper presented at: Proceedings of the 1st  
345 Conference of the Extreme Science and Engineering Discovery Environment: Bridging from  
346 the eXtreme to the campus and beyond (Chicago, IL, USA: Association for Computing  
347 Machinery).

348 Hugall, A.F., Foster, R., Hutchinson, M., and Lee, M.S. (2008). Phylogeny of Australasian  
349 agamid lizards based on nuclear and mitochondrial genes: implications for morphological  
350 evolution and biogeography. *Biological Journal of the Linnean Society* 93, 343-358.

351 Kanehisa, M., and Goto, S. (2000). KEGG: Kyoto Encyclopedia of Genes and Genomes.  
352 *Nucleic Acids Res* 28, 27-30.

353 Kent, W.J. (2002). BLAT--the BLAST-like alignment tool. *Genome Res* 12, 656-664.

354 Kim, D., Paggi, J.M., Park, C., Bennett, C., and Salzberg, S.L. (2019). Graph-based genome  
355 alignment and genotyping with HISAT2 and HISAT-genotype. *Nat Biotechnol* 37, 907-915.

356 Kopylova, E., Noe, L., and Touzet, H. (2012). SortMeRNA: fast and accurate filtering of  
357 ribosomal RNAs in metatranscriptomic data. *Bioinformatics* 28, 3211-3217.

358 Kumar, S., Stecher, G., Suleski, M., and Hedges, S.B. (2017). TimeTree: A Resource for  
359 Timelines, Timetrees, and Divergence Times. *Mol Biol Evol* 34, 1812-1819.

360 Li, H., Handsaker, B., Wysoker, A., Fennell, T., Ruan, J., Homer, N., Marth, G., Abecasis,  
361 G., Durbin, R., and Genome Project Data Processing, S. (2009). The Sequence  
362 Alignment/Map format and SAMtools. *Bioinformatics* 25, 2078-2079.

363 Lieberman-Aiden, E., van Berkum, N.L., Williams, L., Imakaev, M., Ragoczy, T., Telling,  
364 A., Amit, I., Lajoie, B.R., Sabo, P.J., Dorschner, M.O., *et al.* (2009). Comprehensive  
365 mapping of long-range interactions reveals folding principles of the human genome. *Science*  
366 326, 289-293.

367 Lind, A.L., Lai, Y.Y.Y., Mostovoy, Y., Holloway, A.K., Iannucci, A., Mak, A.C.Y., Fondi,  
368 M., Orlandini, V., Eckalbar, W.L., Milan, M., *et al.* (2019). Genome of the Komodo dragon  
369 reveals adaptations in the cardiovascular and chemosensory systems of monitor lizards. *Nat*  
370 *Ecol Evol* 3, 1241-1252.

371 Liu, Y., Zhou, Q., Wang, Y., Luo, L., Yang, J., Yang, L., Liu, M., Li, Y., Qian, T., Zheng, Y.,  
372 *et al.* (2015). Gekko japonicus genome reveals evolution of adhesive toe pads and tail  
373 regeneration. *Nat Commun* 6, 10033.

374 Loytynoja, A., and Goldman, N. (2005). An algorithm for progressive multiple alignment of  
375 sequences with insertions. *Proc Natl Acad Sci U S A* 102, 10557-10562.

376 Luo, R., Liu, B., Xie, Y., Li, Z., Huang, W., Yuan, J., He, G., Chen, Y., Pan, Q., Liu, Y., *et*  
377 *al.* (2012). SOAPdenovo2: an empirically improved memory-efficient short-read de novo  
378 assembler. *Gigascience* 1, 18.

379 Majoros, W.H., Pertea, M., and Salzberg, S.L. (2004). TigrScan and GlimmerHMM: two  
380 open source ab initio eukaryotic gene-finders. *Bioinformatics* 20, 2878-2879.

381 Marcais, G., and Kingsford, C. (2011). A fast, lock-free approach for efficient parallel  
382 counting of occurrences of k-mers. *Bioinformatics* 27, 764-770.

383 Margres, M.J., Rautsaw, R.M., Strickland, J.L., Mason, A.J., Schramer, T.D., Hofmann, E.P.,  
384 Stiers, E., Ellsworth, S.A., Nystrom, G.S., Hogan, M.P., *et al.* (2021). The Tiger Rattlesnake  
385 genome reveals a complex genotype underlying a simple venom phenotype. *Proc Natl Acad*  
386 *Sci U S A* 118.

387 Minh, B.Q., Schmidt, H.A., Chernomor, O., Schrempf, D., Woodhams, M.D., von Haeseler,  
388 A., and Lanfear, R. (2020). IQ-TREE 2: New Models and Efficient Methods for Phylogenetic  
389 Inference in the Genomic Era. *Mol Biol Evol* 37, 1530-1534.

390 Mitchell, A.L., Attwood, T.K., Babbitt, P.C., Blum, M., Bork, P., Bridge, A., Brown, S.D.,  
391 Chang, H.Y., El-Gebali, S., Fraser, M.I., *et al.* (2019). InterPro in 2019: improving coverage,  
392 classification and access to protein sequence annotations. *Nucleic Acids Res* 47, D351-D360.

393 O'Donovan, C., Martin, M.J., Gattiker, A., Gasteiger, E., Bairoch, A., and Apweiler, R.  
394 (2002). High-quality protein knowledge resource: SWISS-PROT and TrEMBL. *Brief*  
395 *Bioinform* 3, 275-284.

396 O'Leary, N.A., Wright, M.W., Brister, J.R., Ciuffo, S., Haddad, D., McVeigh, R., Rajput, B.,  
397 Robbertse, B., Smith-White, B., Ako-Adjei, D., *et al.* (2016). Reference sequence (RefSeq)  
398 database at NCBI: current status, taxonomic expansion, and functional annotation. *Nucleic*  
399 *Acids Res* 44, D733-745.

400 Pepper, M., Barquero, M.D., Whiting, M.J., and Keogh, J.S. (2014). A multi-locus molecular  
401 phylogeny for Australia's iconic Jacky Dragon (Agamidae: *Amphibolurus muricatus*):  
402 Phylogeographic structure along the Great Dividing Range of south-eastern Australia.  
403 *Molecular Phylogenetics and Evolution* 71, 149-156.

404 Peters, R.A., and Evans, C.S. (2003). Introductory tail-flick of the Jacky dragon visual  
405 display: signal efficacy depends upon duration. *Journal of Experimental Biology* 206, 4293-  
406 4307.

407 Quast, C., Pruesse, E., Yilmaz, P., Gerken, J., Schweer, T., Yarza, P., Peplies, J., and  
408 Glockner, F.O. (2013). The SILVA ribosomal RNA gene database project: improved data  
409 processing and web-based tools. *Nucleic Acids Res* 41, D590-596.

410 Roehr, J.T., Dieterich, C., and Reinert, K. (2017). Flexbar 3.0 - SIMD and multicore  
411 parallelization. *Bioinformatics* 33, 2941-2942.

412 Seppey, M., Manni, M., and Zdobnov, E.M. (2019). BUSCO: Assessing Genome Assembly  
413 and Annotation Completeness. *Methods Mol Biol* 1962, 227-245.

414 Smit, A.F., and Hubley, R. (2010). RepeatModeler Open-1.0. 2008-2015. Available at  
415 <http://www.repeatmasker.org>.

416 Song, B., Cheng, S., Sun, Y., Zhong, X., Jin, J., Guan, R., Murphy, R., Che, J., Zhang, Y.,  
417 and Liu, X. (2015a). Anguidae lizard (*Ophisaurus gracilis*) genome assembly data. *Dryad*  
418 *Digital Repository* doi 10, 100119.

419 Song, B., Cheng, S., Sun, Y., Zhong, X., Jin, J., Guan, R., Murphy, R.W., Che, J., Zhang, Y.,  
420 and Liu, X. (2015b). A genome draft of the legless anguid lizard, *Ophisaurus gracilis*.  
421 *Gigascience* 4, 17.

422 Stamatakis, A. (2006). RAxML-VI-HPC: maximum likelihood-based phylogenetic analyses  
423 with thousands of taxa and mixed models. *Bioinformatics* 22, 2688-2690.

424 Stanke, M., Keller, O., Gunduz, I., Hayes, A., Waack, S., and Morgenstern, B. (2006).  
425 AUGUSTUS: ab initio prediction of alternative transcripts. *Nucleic Acids Res* 34, W435-  
426 439.

427 Talavera, G., and Castresana, J. (2007). Improvement of phylogenies after removing  
428 divergent and ambiguously aligned blocks from protein sequence alignments. *Syst Biol* 56,  
429 564-577.

430 Tarailo-Graovac, M., and Chen, N. (2009). Using RepeatMasker to identify repetitive  
431 elements in genomic sequences. *Curr Protoc Bioinformatics* Chapter 4, Unit 4 10.

432 Tian, R., Guo, H., Yang, C., Fan, G., Whiteley, S.L., Holleley, C.E., Seim, I., and Georges,  
433 A. (2021a). Assembled transcriptomes of ovary, testis, and brain (male and female) of  
434 *Amphibolurus muricatus* (jacky dragon) generated using Trinity v2.11.0,  
435 <https://doi.org/10.5281/zenodo.5523684> (Zenodo).

436 Tian, R., Guo, H., Yang, C., Fan, G., Whiteley, S.L., Holleley, C.E., Seim, I., and Georges,  
437 A. (2021b). Draft de novo genome assemblies of a male and female *Amphibolurus muricatus*  
438 (jacky dragon), <https://doi.org/10.5281/zenodo.5523788> (Zenodo).

439 Tian, R., Guo, H., Yang, C., Fan, G., Whiteley, S.L., Holleley, C.E., Seim, I., and Georges,  
440 A. (2021c). Gene annotations of *Amphibolurus muricatus* (jacky dragon), *Intellagama*  
441 *lesueurii* (Australian water dragon), *Phrynocephalus przewalskii* (Przewalski's toadhead  
442 agama), and *Phrynocephalus vlangalii* (Ching Hai toadhead agama),  
443 <https://doi.org/10.5281/zenodo.5523656> (Zenodo).

444 UniProt Consortium (2012). Reorganizing the protein space at the Universal Protein  
445 Resource (UniProt). *Nucleic Acids Res* 40, D71-75.

446 Vurture, G.W., Sedlazeck, F.J., Nattestad, M., Underwood, C.J., Fang, H., Gurtowski, J., and  
447 Schatz, M.C. (2017). GenomeScope: fast reference-free genome profiling from short reads.  
448 *Bioinformatics* 33, 2202-2204.

449 Wang, O., Chin, R., Cheng, X., Wu, M.K.Y., Mao, Q., Tang, J., Sun, Y., Anderson, E., Lam,  
450 H.K., Chen, D., *et al.* (2019). Efficient and unique cobarcoding of second-generation  
451 sequencing reads from long DNA molecules enabling cost-effective and accurate sequencing,  
452 haplotyping, and de novo assembly. *Genome Res* 29, 798-808.

453 Warner, D., and Shine, R. (2008). The adaptive significance of temperature-dependent sex  
454 determination in a reptile. *Nature* 451, 566-568.

455 Warner, D.A., Uller, T., and Shine, R. (2013). Transgenerational sex determination: the  
456 embryonic environment experienced by a male affects offspring sex ratio. *Scientific reports*  
457 3, 1-4.

458 Warren, R.L., Yang, C., Vandervalk, B.P., Behsaz, B., Lagman, A., Jones, S.J., and Birol, I.  
459 (2015). LINKS: Scalable, alignment-free scaffolding of draft genomes with long reads.  
460 *Gigascience* 4, 35.

461 Weisenfeld, N.I., Kumar, V., Shah, P., Church, D.M., and Jaffe, D.B. (2017). Direct  
462 determination of diploid genome sequences. *Genome Res* 27, 757-767.

463 Whiteley, S.L., Georges, A., Weisbecker, V., Schwanz, L.E., and Holleley, C.E. (2021).  
464 Ovotestes suggest cryptic genetic influence in a reptile model for temperature-dependent sex  
465 determination. *Proceedings of the Royal Society B* 288, 20202819.

466 Woo, K., and Rieucan, G. (2013). Efficiency of aggressive and submissive visual displays  
467 against environmental motion noise in Jacky dragon (*Amphibolurus muricatus*). *Ethology*  
468 *Ecology & Evolution* 25, 82-94.

469 Xue, W., Li, J.T., Zhu, Y.P., Hou, G.Y., Kong, X.F., Kuang, Y.Y., and Sun, X.W. (2013).  
470 L\_RNA\_scaffolder: scaffolding genomes with transcripts. *BMC Genomics* 14, 604.

471 Yang, Z. (2007). PAML 4: phylogenetic analysis by maximum likelihood. *Mol Biol Evol* 24,  
472 1586-1591.

473 Zheng, G.X., Lau, B.T., Schnall-Levin, M., Jarosz, M., Bell, J.M., Hindson, C.M.,  
474 Kyriazopoulou-Panagiotopoulou, S., Masquelier, D.A., Merrill, L., Terry, J.M., *et al.* (2016).  
475 Haplotyping germline and cancer genomes with high-throughput linked-read sequencing. *Nat*  
476 *Biotechnol* 34, 303-311.

477 Zhu, B.H., Xiao, J., Xue, W., Xu, G.C., Sun, M.Y., and Li, J.T. (2018). P\_RNA\_scaffolder: a  
478 fast and accurate genome scaffolder using paired-end RNA-sequencing reads. *BMC*  
479 *Genomics* 19, 175.

480

481

482 **Figure legends**



483

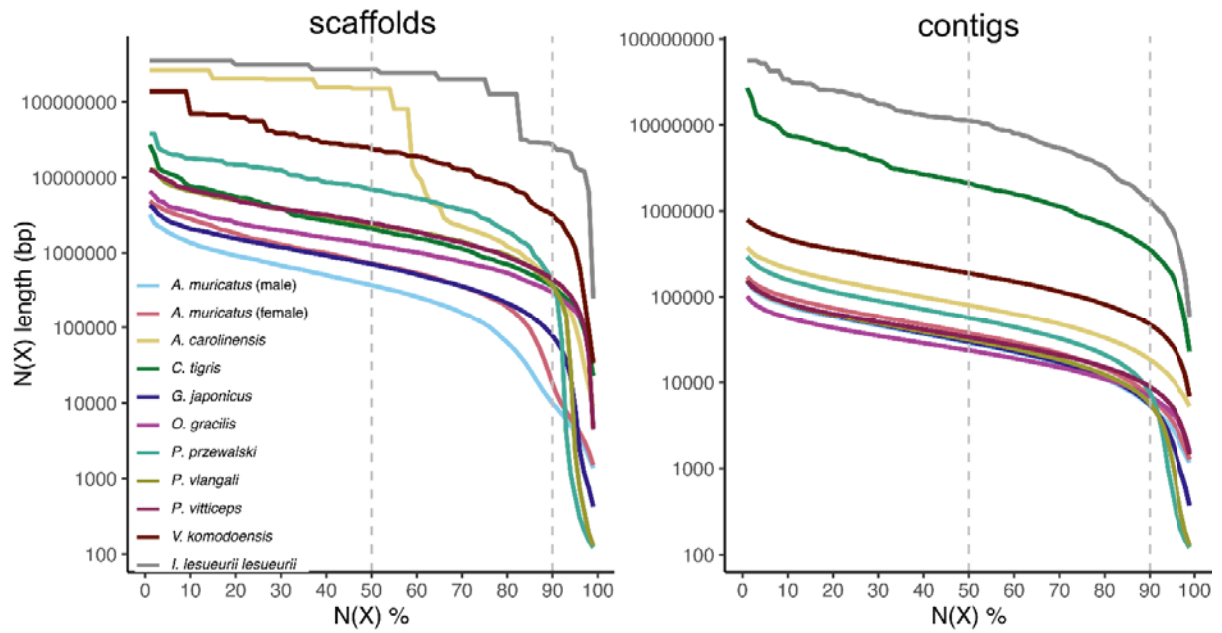
484 **Figure 1** Photograph of an adult male jacky dragon (*Amphibolurus muricatus*). Image credit:

485 David Cook Wildlife Photography.

486

487



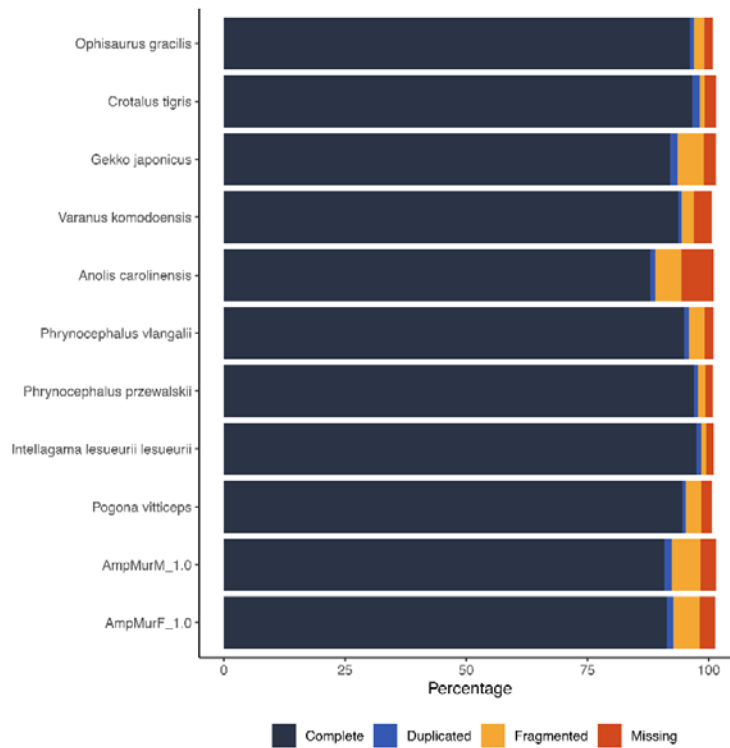


488

489 **Figure 2** Comparison of the contiguity of two *A. muricatus* assemblies and nine publicly  
 490 available squamate assemblies. N(x)% graphs show the (A) contig and (B) scaffold lengths  
 491 (y-axis), where x% (x-axis) of the genome assembly consist of scaffolds and contigs of at  
 492 least that size. Dashed, grey lines denote N50 and N90 values.

493





495

496 **Figure 3** BUSCO assessment of assemblies from ten squamate species. All genome  
 497 assemblies were examined using the same version and library of BUSCO (5.0.0\_cv1 with the  
 498 3,354-gene vertebrata\_odb10 dataset). AmuF\_1.1 and AmuM\_1.1 denotes the female and  
 499 male *A. muricatus* assembly, respectively.

500

501

502

503

504

505

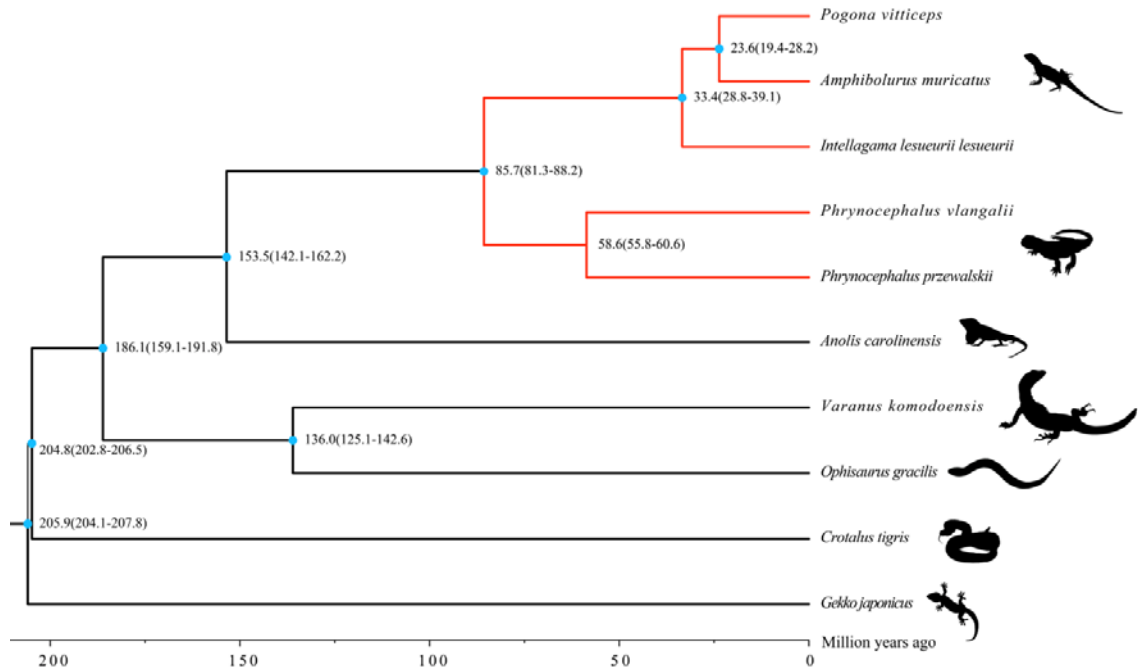
506

507

508

509

510



511

512 **Figure 4** Inferred phylogeny of ten squamate species based on whole-coding sequences of  
 513 4,242 1:1 orthologs. Numbers at nodes represent the estimated divergence time from present  
 514 (million years ago; Mya) between lineages. Agamid (family Agamidae) lineages are indicated  
 515 in red.

516

517

518

519 **Tables**520 **Table 1** *A. muricatus* genome assembly statistics. Lengths in base pairs (bp).

<b>Assembly methods</b>	<b>Female (AmuF.1.1)</b>	<b>Male (AmuM.1.1)</b>
Contig number	124,200	151,787
Contig length	1,750,545,991	1,741,048,453
Contig N50 (bp)	37,220	28,761
Contig max length	348,284	288,200
Scaffold number	57,227	73,856
Scaffold length	1,841,491,868	1,833,283,242
Scaffold N50 (bp)	720,518	369,860
Scaffold max length	6,534,950	6,446,322
Gaps (bp)	90,945,877	92,234,789
Gaps (%)	4.94	5.03
GC content (%)	41.77	41.70

521